Developmental Biology 347 (2010) 180–194

Contents lists available at ScienceDirect

Developmental Biology

journal homepage: www.elsevier.com/developmentalbiology

Sumoylation controls retinal progenitor proliferation by repressing cell cycle exit in *Xenopus laevis*

Koji Terada [a], Takahisa Furukawa [a,b,*]

[a] Department of Developmental Biology, Osaka Bioscience Institute, 6-2-4 Furuedai, Suita, Osaka 565-0874, Japan
[b] JST, CREST, 6-2-4 Furuedai, Suita, Osaka 565-0874, Japan

ARTICLE INFO

Article history:
Received for publication 14 June 2010
Revised 7 August 2010
Accepted 20 August 2010
Available online 27 August 2010

Keywords:
Ubc9
Sumo
Xenopus
Retina
Cell cycle
Progenitor

ABSTRACT

Precisely controlled progenitor proliferation is essential for normal development. However, molecular mechanisms, which control the correct timing of cell cycle withdrawal during development, have been poorly understood. We show here that ubc9, a sumo-conjugating enzyme, controls the cell cycle exit of retinal progenitors. We found that *ubc9* is highly expressed in retinal progenitors and stem cells in *Xenopus* embryos. Ubc9 physically and functionally associates with *Xenopus* hmgb3, which is required for retinal cell proliferation, and prolonged expression of ubc9 and hmgb3 results in suppression of the cell cycle exit of retinal progenitors in a sumoylation-dependent manner. Overexpression of *ubc9* and *hmgb3* decreased expression of the cell-cycle inhibitor $p27^{Xic1}$. Furthermore, progenitor proliferation is regulated, at least in part, by sumoylation of transcription factor Sp1. These results suggest a significant role of sumoylation for cell cycle regulation in retinal progenitors.

Introduction

The vertebrate neural retina is a complex sensory tissue whose function depends on the production of a sufficient number of cells of each retinal cell type and the correct formation of laminar cytoarchitecture. The seven major cell types that compose the neural retina arise from a pool of multipotent progenitors (Young, 1985; Cepko et al., 1996). Birthdating studies have demonstrated that the seven retinal cell types are generated in an evolutionarily conserved order during development, although multiple cell types are simultaneously produced at any given developmental stage (Cayouette et al., 2006; Cepko et al., 1996). Therefore, retinal progenitor cells stop proliferation to differentiate into the cell types that are generated earlier, but also proliferate extensively at an appropriate rate to produce a sufficient number of later cell types. Thus, cell proliferation and cell differentiation occur in parallel in the developing vertebrate retina (Cepko et al., 1996; Donovan and Dyer, 2005; Harris, 2009; Levine and Green, 2004; Young, 1985). A number of extrinsic cues, including Wnt, Hedgehog and Notch signaling pathways have been implicated in the control of retinal progenitor proliferation and differentiation in the developing retina (Denayer et al., 2008; Dorsky et al., 1997; Van Raay et al., 2005; Wallace, 2008). On the other hand, the significance of the cell-intrinsic program has been suggested by the clonal density culture of retinal progenitor cells from the rat retina at embryonic day 17.5 (E17.5) (Cayouette et al., 2003). A number of homeodomain transcription factors have been implicated in the control of retinal progenitor proliferation, including *rax*/*Rx*, *Pax6*, *Chx10*, *Six3*, *six6*/*optx2* and *Prox1*. They are involved in the regulation of cell fate competency, cell proliferation and cell differentiation of retinal progenitors (Burmeister et al., 1996; Casarosa et al., 2003; Dyer et al., 2003; Furukawa et al., 2000; Green et al., 2003; Li et al., 2002; Marquardt et al., 2001; Zuber et al., 1999). However, molecular mechanisms controlling the balance of two opposing cell behaviors, cell proliferation and cell cycle exit during development, remain to be elucidated.

Cyclin-dependent kinase inhibitors (CKI) play a significant role in the regulation of the cell cycle. Two families of Cdk inhibitors, the Cip/Kip family, which includes $p27^{Kip1}$, $p21^{Cip1}$ and $p57^{Kip2}$, and the Ink4 family, comprised of $p16^{Ink4a}$, $p15^{Ink4b}$, $p18^{Ink4c}$ and $p19^{Ink4d}$, have been identified. CKI can inhibit the various cyclin-Cdk complexes that control G1 progression and entry into the S phase, and its overexpression in various cell lines arrests the cell cycle in G1 (Besson et al., 2008; Sherr and Roberts, 1999). In mice $p27^{Kip1}$ regulates the cell cycle withdrawal of late retinal progenitor cells, and in *Xenopus* $p27^{Xic1}$ regulates cell cycle exit and Müller glia development in the developing retina (Levine et al., 2000; Ohnuma et al., 1999).

Sumoylation is a highly conserved evolutionary pathway, from yeast to vertebrates. Ubc9 is the only known small ubiquitin-related modifier (sumo) E2-conjugating enzyme. In *Saccharomyces cerevisiae*, *ubc9* depletion results in cell cycle arrest at the G2/M phase (Seufert et al., 1995). By contrast, in *Schizosaccharomyces pombe*, the *hus5*

* Corresponding author. Department of Developmental Biology, Osaka Bioscience Institute, 6-2-4 Furuedai, Suita, Osaka 565-0874, Japan. Fax: +81 6 6872 3933.
E-mail address: furukawa@obi.or.jp (T. Furukawa).

0012-1606/$ – see front matter © 2010 Elsevier Inc. All rights reserved.
doi:10.1016/j.ydbio.2010.08.023

(ubc9 homolog) deletion mutant is viable, however, the cells exhibit high levels of abortive mitosis and chromosome missegregation (al-Khodairy et al., 1995). RNAi-mediated knockdown of *ubc9* in *Caenorhabditis elegans* results in embryonic arrest after gastrulation and pleiotropic defects in larval development such as vulval eversion at the fourth larval stage and abnormal tail morphology (Jones et al., 2002). In *Drosophila melanogaster*, the *ubc9* lethal mutant, known as *lesswright*, dominantly suppresses the nondisjunction and cytological defects of female meiotic mutations that affect spindle formation (Apionishev et al., 2001). In zebrafish, ubc9 regulates mitosis and cell survival during development. Loss of *ubc9* leads to compromised mitosis and cellular overgrowth, and *ubc9* is required for tissue-specific cell viability in zebrafish (Nowak and Hammerschmidt, 2006). In mice, the ubc9-mediated sumo pathway is essential for nuclear integrity and chromosome segregation (Nacerddine et al., 2005). Sumo post-translationally modifies many proteins with roles in diverse processes including regulation of transcription, chromatin structure, DNA repair, protein localization, and protein activity (Geiss-Friedlander and Melchior, 2007; Hay, 2005; Johnson, 2004). It was reported that neural crest precursor formation is regulated by sumoylation of SoxE in *Xenopus*, resulting in a change in the physiological role of the SoxE protein (Taylor and Labonne, 2005). Recently, it was also reported that sumoylation has an important role in retinal photoreceptor differentiation (Onishi et al., 2009). However, the exact role of *ubc9* in retinal development remains to be elucidated.

Rax/Rx is a transcription factor that is predominantly expressed in retinal progenitors and is essential for eye development in vertebrates (Furukawa et al., 1997; Mathers et al., 1997). *Rax* is conserved among species, including human, mouse, chicken, fish and *Xenopus*. We previously demonstrated that *Xenopus* high mobility group box 3 (*hmgb3*) is one of the downstream factors of rax (Terada et al., 2006). Overexpression and loss-of-function experiments have indicated that *hmgb3* has a significant role in retinal progenitor proliferation during eye development in *Xenopus*. Hmgb3 is an evolutionally conserved nuclear protein without a transactivation domain and has been thought to function as a chromatin modulator, suggesting that hmgb3 functions through a protein complex. In the current study, we identified ubc9, a sumo conjugating enzyme, to be an interacting partner of hmgb3. We demonstrated that ubc9 regulates retinal progenitor proliferation in a hmgb3-dependent manner, at least in part, via the suppression of $p27^{Xic1}$ expression through Sp1 sumoylation. Our results suggest that protein sumoylation plays an important role in controlling retinal progenitor proliferation.

Materials and methods

Yeast two-hybrid assays

We carried out a yeast two-hybrid screen using MATCHMAKER GAL4 Two-Hybrid System 3 (Clontech). The *AH109* yeast strain bearing the bait plasmid *pGBKT7-hmgb3* was transformed with the mouse retinal (Postnatal day 0 (P0)-P3) cDNA library in a *pGADT7* vector. Initially, about 400,000 clones were screened. Yeast colonies that grew at 30 °C on SD-Trp-Leu-His were re-streaked on SD-Trp-Leu-His-Ade (218 colonies). Streaked yeast colonies that grew on SD-Trp-Leu-His-Ade (121 colonies) were subjected to the β-galactosidase (β-gal) assay. 24 colonies were positive in the β-gal assay. Rescued plasmids from yeast into *Escherichia coli* strain *DH5α* were classified by enzyme digestion pattern. Each representative plasmid was re-introduced into the yeast strain *AH109* together with *pGBKT7-hmgb3* to confirm the reproducibility and specificity of interactions. Seven clones were obtained and six of them were *ubc9* cDNAs. The amino acid sequences of mouse ubc9 and *Xenopus* ubc9 are identical. Therefore, the mouse *ubc9* cDNA was used for overexpression experiments using *Xenopus* embryos.

Embryo manipulations

Embryos were obtained from *Xenopus laevis* adult frog by hormone-induced egg laying and *in vitro* fertilization. Embryos were staged according to Nieuwkoop and Faber (1994). Glucocorticoid receptor fusion proteins were activated by adding 25 μM dexamethasone (DEX) (Sigma, D1756) into the culture medium. Injected embryos were raised at 15 °C. *Xenopus* embryos were abdominally injected with 5-Bromo-2'-deoxy-uridine (BrdU) (20 mM) for BrdU labeling.

RNA synthesis and RNA microinjection

Capped RNAs were synthesized using the MESSAGE mMACHINE kit (Ambion). One animal dorsal blastomere was injected for phenotype observations at the 8-cell stage. The amount of injected synthetic RNAs were as follows; 75 pg of *lacZ*, 100 pg of *EGFP*, 225 pg of *hmgb3*, 250 pg of *hmgb3* (*mut*), 100 pg of *ubc9*, 200–800 pg of *ubc9* (*C93A*), 200 pg or 400 pg of *sumo-Sp1-GR*, 800 pg of *Sp1(17-723)-GR*, 400 pg of *Sp1-GR*.

X-gal staining and in situ hybridization

Embryos were grown to a desired stage and fixed in MEMFA (0.1 M MOPS (pH 7.4), 2 mM EGTA, 1 mM $MgCl_2$, 3.7% formaldehyde) for 30 min and transferred into the X-gal staining solution until staining was apparent. *In situ* hybridization was performed essentially as described (Harland, 1991). RNA probes of *Xenopus hmgb3* and *Xenopus rax* were previously described (Terada et al., 2006).

Quantification of enlarged eye size

Embryos injected with synthetic RNA were grown to stage 37/38 and fixed in MEMFA followed by X-gal staining. Quantification of enlarged eye was performed as previously described (Terada et al., 2006). The eye diameters were measured by Image J and used to calculate the percent increase in eye diameter on the injected side to the un-injected side. The epidermis overlaying the eye was removed.

Animal cap dissections

Animal caps were dissected from stage 8/9 embryos in 0.5x MMR (Marc's Modified Ringer's solution). The caps were incubated until sibling embryos reached stage 19/20 and then subjected to further analysis.

Immunohistochemistry

Immunostaining of frozen sections was performed essentially as described previously with minor modifications (Terada et al., 2006). A blocking solution containing 0.2% of TritonX-100 was used. Sections were incubated for 1 h in 2N HCl prior to BrdU immunodetection. For immunostaining, anti-β-galactosidase (β-gal) antibody (Promega, #Z3781), anti-phospho-histone H3 antibody (Upstate, #06-570), anti-BrdU antibody (Fitzgerald, #20-BS17), anti-calbindin (calbiochem #PC253L), anti-islet1 (DSHB, clone 39.4D5), and anti-PCNA antibody (DAKO, M0879) were used for primary antibodies, Cy3-conjugated-anti-rabbit IgG (Jacson ImmunoResearch Laboratories, #711-165-152), Cy3-conjugated-anti-mouse IgG (Jacson ImmunoResearch Laboratories, #711-165-150), Alexa Fluor 488-conjugated-anti-sheep IgG (Invitrogen, #A11015) and Alexa Fluor 488-conjugated-anti-mouse IgG (Invitrogen, #A11001) were used for secondary antibodies. For immunoprecipitation and Western blots, anti-HA antibody (Santa Cruz, #sc-805), anti-myc antibody (Santa Cruz, #sc-40), anti-FLAG antibody (M2) (Sigma, #F3165) were used.

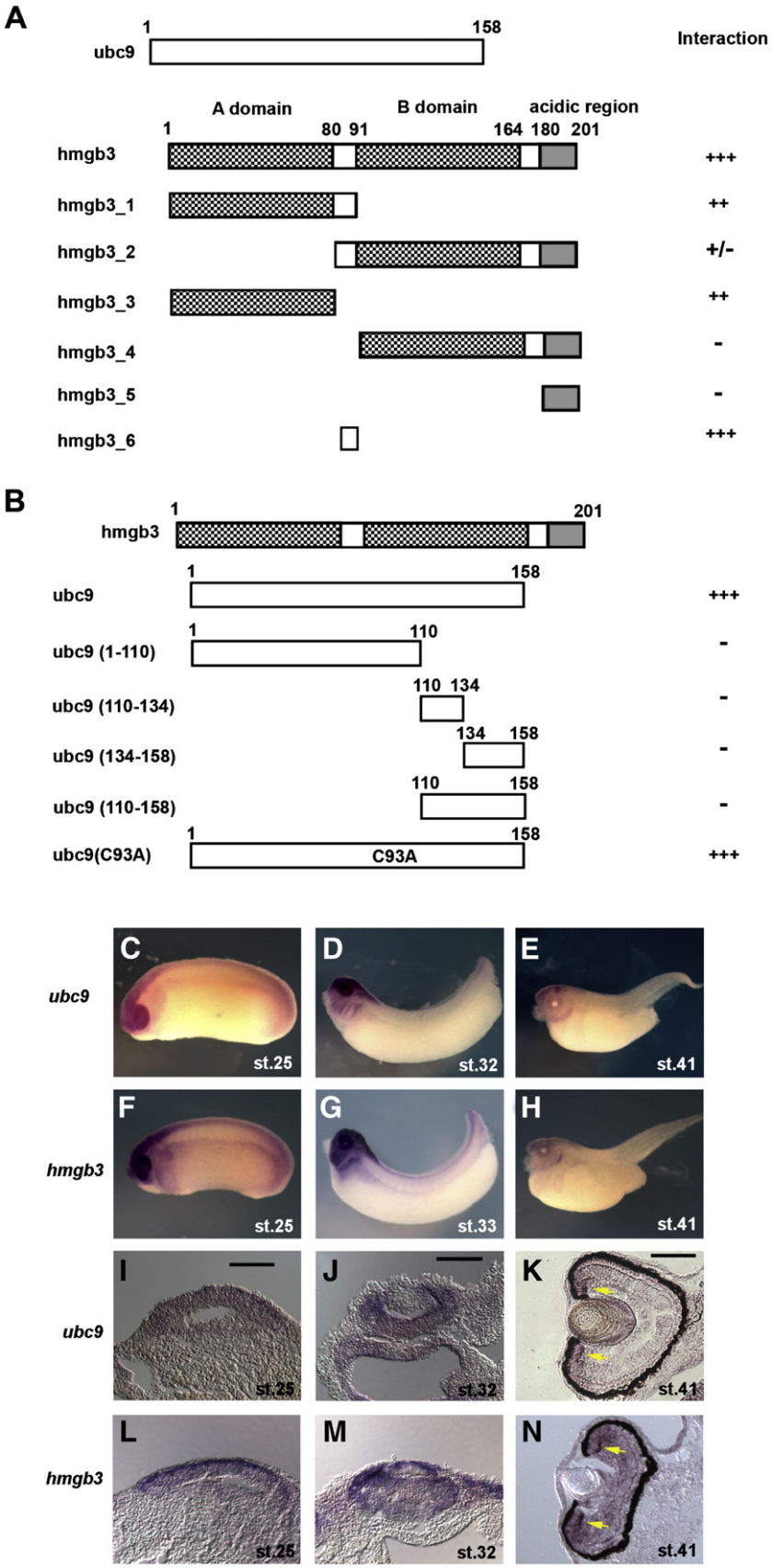

Fig. 1. Ubc9 interacts with hmgb3, and *ubc9* mRNA shows a similar expression pattern with that of *hmgb3* mRNA. (A, B) Analysis of interaction between hmgb3 and ubc9 by yeast two-hybrid assay. Strength of interaction of deletion constructs of hmgb3 (A) or ubc9 (B) are represented. +++, ++, + reflect on the extent of the ability to grow on medium lacking adenine and histidine. (C–N) Expression of *ubc9* and *hmgb3* in developing *Xenopus* embryos. Expression of *ubc9* (C–E, I–K) or *hmgb3* (F–H, L–N) was analyzed by whole mount *in situ* hybridization (C–H) followed by producing the frozen sections (I–N) at stages indicated in each panel. *Ubc9* or *hmgb3* is expressed in the optic vesicle (I, L), in the developing retina (J, M), and in the CMZ in the post embryonic retina as indicated by yellow arrows (K, N). Scale bar, 100 μm.

In vivo lipofection

DNA was lipofected into the anterior neural fold of stage 18 embryos as previously described (Dorsky et al., 1997). *EGFP* DNA was co-lipofected to mark the lipofected cells. Embryos were fixed at stage 41 and sectioned at a thickness of 10 μm. EGFP-positive cells were counted and the cell type was identified based upon their laminar position and morphology as previously described (Dorsky et al., 1997).

Analysis of nuclear density, cell death, and BrdU-positive or phospho-histone H3 (pH3)-positive cells

Embryos were harvested at stages 32/33, 33/34, 35/36, 40 or 41 and fixed in MEMFA. Cryosections (10 μm) were made from embryos and subjected to nuclear density analysis (stage 40), TUNEL (TdT-mediated dUTP Nick-End Labeling) assay (stage 33/34 or 35/36) using the *in situ* Apoptosis Detection Kit (TAKARA), immunostaining for BrdU (stages 40 and 41) or for pH3 (stage 32/33 and stage 33/34).

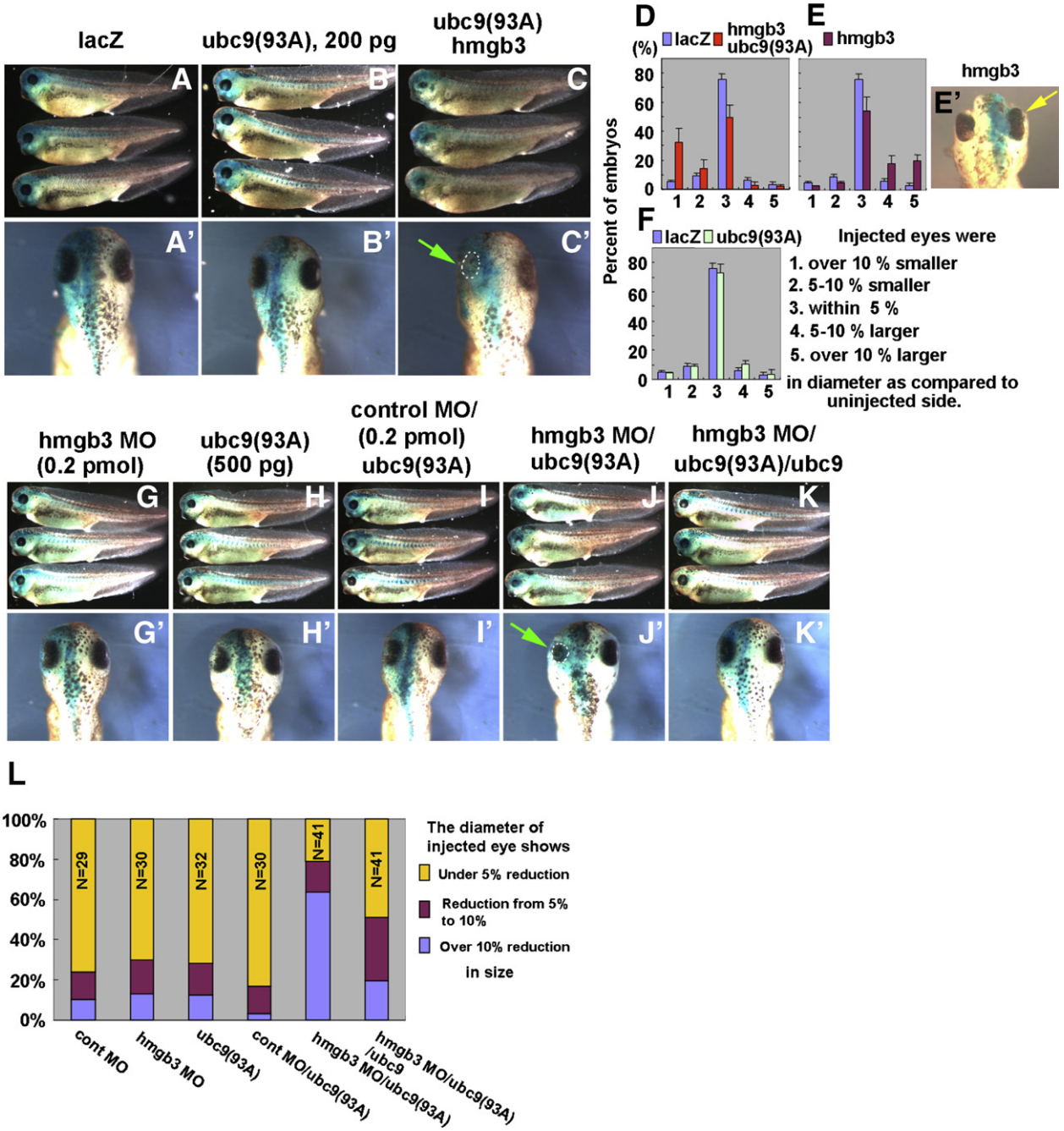

Fig. 2. Ubc9 and hmgb3 are functionally associated in eye development in *Xenopus*. (A–L) *Xenopus* embryos were injected with synthetic RNAs or morpholino oligos as indicated above each panel (A–C, E', G–K), and harvested at stage 37/38 followed by X-gal staining. Embryos are represented as lateral views with anterior to the left (A–C, G–K) and as dorsal view with anterior to the top (A'–C', E', and G'–K'). Injected side is indicated by β-gal activity in blue (A–C', E', G–K'). Diameters of the eyes of each embryo were compared between the injected side and the uninjected side (D–F, L). Data are means from three experiments with the numbers indicated as follows ± s.e.m. (D–F). The numbers of embryos analyzed (n) and the mean of the ratio of eye size between injected side and uninjected side (r): *lacZ*, $(n, r) = (31, 1), (30, 0.99), (34, 1)$ (D–F), *lacZ*, *ubc9 (93A)* plus *hmgb3*, $(n, r) = (31, 0.94), (31, 0.93), (31, 0.88)$ (D), *lacZ*/*hmgb3*, $(n, r) = (34, 1.06), (36, 1.02), (32, 1.05)$ (E) and *lacZ*/*ubc9 (93A)*, $(n, r) = (36, 1), (31, 0.99), (33, 0.99)$ (F). Differences in eye diameter between the injected side and the uninjected side were classified as indicated in the right side of (F) and the ratio of each class to the total number are indicated (D–F). Differences in eye diameter between the injected side and the uninjected side were classified as indicated at the right side and the ratio of each class to the total number is indicated (L). Green arrows indicate reduced eye size (C', J'). Yellow arrow indicates the enlarged eye (E').

DAPI-positive cells in an arbitrary unit area (in the inner nuclear layer) were counted and cell density was calculated. TUNEL assay was performed according to the instruction manual protocol. The number of apoptotic cells and DAPI-positive signals were counted, and percentages of apoptotic cells were calculated. The number of BrdU-positive cells and DAPI-positive signals were counted, and percentages of BrdU-positive cells were calculated (stage 32/33) or BrdU-positive cells were counted (stages 40 and 41). To examine the ratio of the number of pH3-positive cells to the total number of cells, the number of pH3-positive cells and DAPI-positive signals were counted, and percentages of pH3-positive cells were calculated. To examine the ratio of the number of BrdU-labeled cells to the total number of cells,

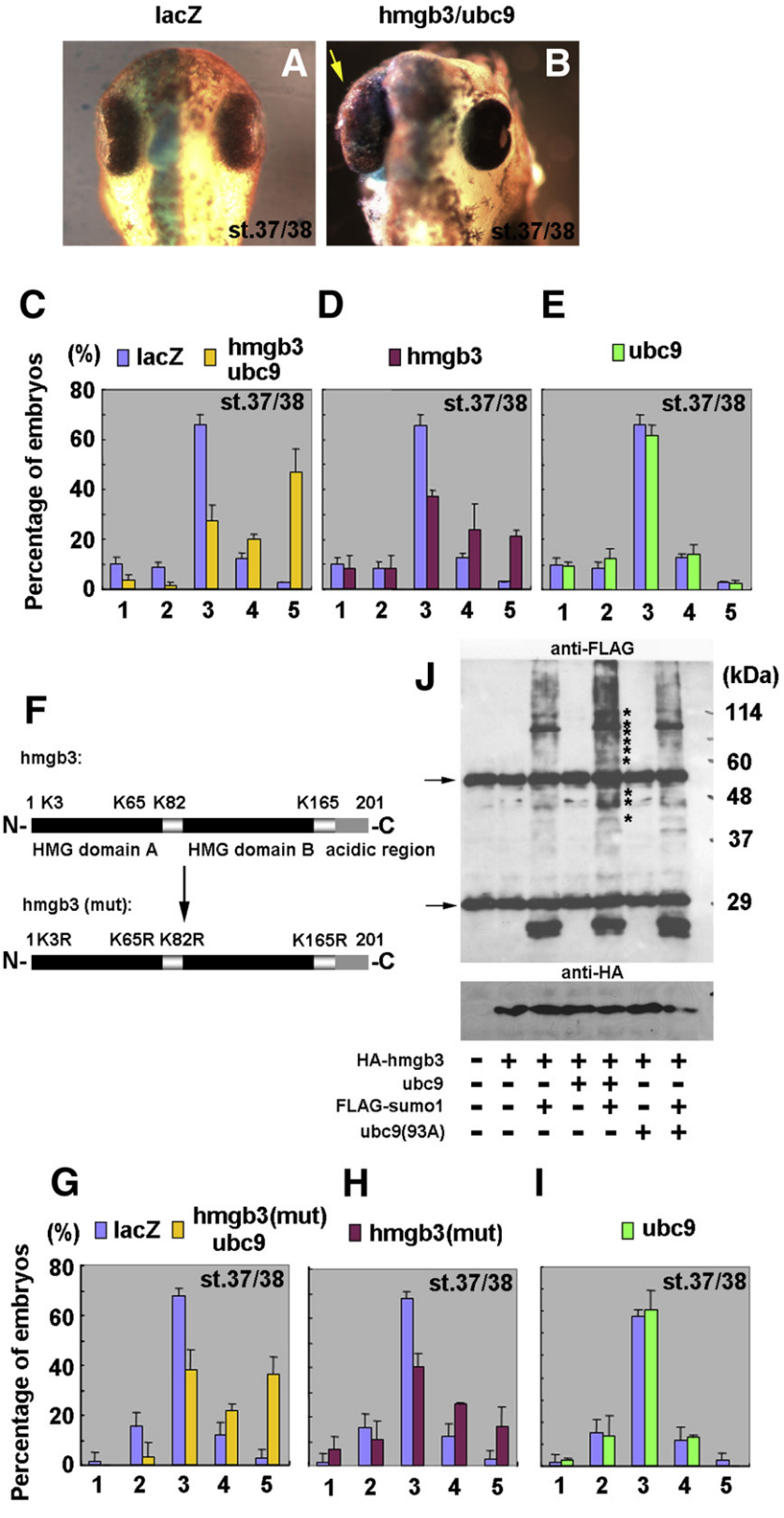

three adjacent serial sections corresponding to the central retina were prepared. One of the these sections was stained with an anti-BrdU antibody, one was stained with DAPI, and the third was stained with an anti-β-gal antibody, since HCl treatment makes DAPI staining of nucleus and anti-β-gal staining inefficient. The serial sections in which almost all retinal cells were stained with an anti-β-gal antibody were used for subsequent analysis. Each analysis was conducted on three to nine eyes for each experiment, and for each eye the average value was calculated from two to three sections.

Analysis of cell differentiation by immunohistochemistry of BrdU-incorporating cells in the developing retina

Embryos injected with *lacZ* or *lacZ*/*ubc9*/*hmgb3* RNAs at the eight cell stage were injected with BrdU at stage 40/41. Injected embryos were raised to stage 46 and harvested. Retinal sections were co-immunostained with an anti-BrdU antibody and antibodies to retinal neuron markers. Image acquisition and analysis of the signals obtained were performed using Zeiss Confocal LSM510 Microscope.

Immunoprecipitation assay, sumoylation assay and Western blots

293T cell lysates or *Xenopus* embryo lysates, which were injected with synthetic RNAs, were prepared in immunoprecipitation (IP) buffer (50 mM Tris•HCl, pH 7.5, 1 mM EDTA, 2 mM $MgCl_2$, 150 mM NaCl, 1 mM Phenylmethylsulfonyl fluoride, 0.5% TritonX-100) in the presence of protease inhibitor tablets (Roche) and spun at 17,400*g* for 10 min at 4 °C. N-ethylmaleimide was added (20 mM) to IP buffer when sumoylation of proteins were detected. The indicated antibodies and Protein G sepharose (Amersham) were added to the supernatants, and incubated at 4 °C overnight. The sepharose beads were washed five times with IP buffer. Western blots were performed with indicated antibodies.

Real-time PCR

Total RNA was reverse-transcribed by Superscript II (Invitrogen) using random primers. Real-time PCR was performed using the Thermal Cycler Dice Real Time System (TAKARA) and SYBR GreenER qPCR SuperMix Universal (Invitrogen), according to the manufacturer's protocols. Quantified RNA values were normalized with those of ribosomal RNA. Quantitative analysis was performed at least three times and shown with standard errors.

Plasmids and PCR primers

Details of plasmid construction and the primer sequences used for plasmid construction are available upon request.

Results

Ubc9 is expressed in the developing CNS in Xenopus embryos

We previously found that *hmgb3* is essential for proliferation of retinal progenitors (Terada et al., 2006). In the current study we performed a yeast two-hybrid screen to identify a factor(s) that interacts with hmgb3 protein in the context of retinal development. A full-length hmgb3 coding sequence, fused in-frame to the yeast Gal4 DNA binding domain was expressed in the *AH109* strain and this yeast strain was used to screen a mouse retinal cDNA library fused with the Gal4 activation domain. In this screen we identified ubc9 as an interacting protein with hmgb3 (Fig. 1A, B). To confirm the specificity of hmgb3-ubc9 association, as well as to identify the region(s) of hmgb3 responsible for the interaction, we constructed a series of hmgb3 deletion mutants in the *pGBKT7* vector (Fig. 1A) and expressed each of these in *AH109* yeast transformed with *pGADT7-ubc9*. The ability to grow on medium lacking adenine and histidine revealed that hmgb3 has a ubc9-interacting domain in the N-terminal region (1-91 amino acids). We named this mutant hmgb3_1 (Fig. 1A). To identify the region of ubc9 responsible for its interaction with the hmgb3 protein, we pursued a deletion-based interaction assay (Fig. 1B). We observed that ubc9(93A), which is a inactive form of ubc9, can bind to hmgb3, suggesting that enzymatic activity is not required for ubc9 to bind to hmgb3 (Fig. 1B). All partial fragments of ubc9 failed to interact with hmgb3, suggesting that a full-length ubc9 is required for interaction with hmgb3. We also detected ubc9 and hmgb3 interaction by co-immunoprecipitation assay using 293T cells transfected with *ubc9* and *hmgb3* expression constructs (Supplementary Fig. S1). We then analyzed the expression pattern of *ubc9* in developing *Xenopus* embryos, and found that *ubc9* is expressed mainly in the developing central nervous system (CNS) including the developing retina (Fig. 1C–E, I, J). In the developing retina, *ubc9* appeared to be expressed in retinal progenitors (Fig. 1I, J) and restricted to the CMZ, where retinal stem cells reside, as development proceeded (Fig. 1K). Thus, the expression pattern of *ubc9* was similar to that of *hmgb3* in *Xenopus* embryonic development (Fig. 1C–N) (Terada et al., 2006).

Ubc9 and hmgb3 are functionally associated in retinal development

We focused our analysis on the retina in the current study, although *ubc9* is expressed ubiquitously in the developing *Xenopus* CNS. *Ubc9* has been reported to be expressed in the progenitor/stem cells in the developing rat CNS as well (Watanabe et al., 2008), however, the roles of ubc9 in progenitor/stem cells in the rat CNS are unknown. Thus, we investigated a possible role of ubc9 in retinal progenitor/stem cells by taking advantage of the *Xenopus* system so that we can perform overexpression and/or loss-of-function experiments on several genes simultaneously in order to evaluate functional interactions between genes of interest.

We first tested whether or not *ubc9* sumoylation activity is required for *hmgb3* to induce eye enlargement using a sumoylation activity-

Fig. 3. Ubc9 and hmgb3 function synergistically in a hmgb3 sumoylation-independent manner. (A–E) Overexpression of *lacZ* alone (A, C–E), *lacZ*/*ubc9*/*hmgb3* (B, C), *lacZ*/*hmgb3* (D) or *lacZ*/*ubc9* (E) in *Xenopus* embryos. Embryos were harvested at stage 37/38 (A–E) and injected side is indicated by β-gal activity in blue (A, B). Yellow arrow indicates the enlarged eye (B). Diameters of the eyes were compared between the injected side and the uninjected side (C–E). Differences in eye diameter between the injected side and the uninjected side were classified as indicated in the right side of Fig. 2F, and the ratio of each class to the total number are indicated (C–E). Data are means from three experiments with the numbers indicated as follows ± s.e.m. (C–E). The numbers of embryos analyzed (n) and the mean of the ratio of eye size between injected side and uninjected side (r): *lacZ*, (n, r) = (32, 0.96), (31, 0.99), (38, 0.99) (C–E), *lacZ*, *ubc9* plus *hmgb3*, (n, r) = (32, 1.12), (36, 1.09), (41, 1.07) (C), *lacZ*/*hmgb3*, (n, r) = (31, 1.04), (31, 0.99), (38, 1.06) (D), *lacZ*/*ubc9*, (n, r) = (20, 1), (26, 0.98), (45, 1) (E). (F) The structure of *hmgb3* and *hmgb3 (mut)*. Lysine residues with a high probability of sumoylation are represented. Four lysine residues were substituted with arginine residues (hmgb3 (mut)). (G–I) Overexpression of *lacZ* alone (G-I), *lacZ*/*ubc9*/*hmgb3 (mut)* (G), *lacZ*/*hmgb3 (mut)* (H) or *lacZ*/*ubc9* (I) in *Xenopus* embryos. Embryos were harvested at stage 37/38 (G–I). The effects of genes of interest were analyzed as in C–E (G–I). Data are means from three experiments with the numbers indicated as follows ± s.e.m. (G–I). The numbers of embryos analyzed (n) and the mean of the ratio of eye size between injected side and uninjected side (r): *lacZ*, (n, r) = (35, 0.98), (35, 0.99), (33, 1) (G-I), *lacZ*/*ubc9*/*hmgb3 (mut)*, (n, r) = (37, 1.09), (32, 1.06), (30, 1.07) (G), *lacZ*/*hmgb3 (mut)*, (n, r) = (36, 1.05), (34, 1.02), (32, 1) (H), and *lacZ*/*ubc9*, (n, r) = (35, 1), (33, 0.99), (31, 1) (I). (J) Embryos were injected with synthetic RNAs of indicated and harvested at stage 28 followed by an immunoprecipitation (IP) assay using an anti-FLAG antibody, SDS-PAGE and Western blot analysis using an anti-FLAG antibody. Lysates of embryos were aliquoted before IP and used for SDS-PAGE, Western blotting, and probed with an anti-HA peptide antibody as a loading control. Asterisks indicate sumoylated bands. Arrows indicate the heavy chain and light chain of mouse IgG.

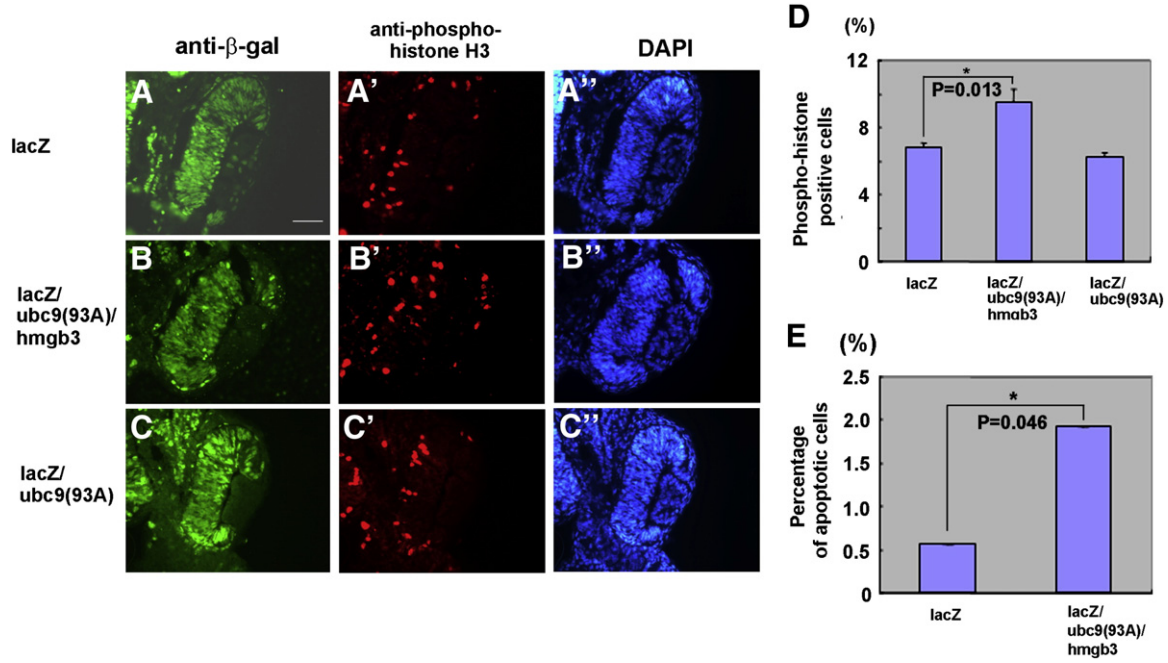

Fig. 4. The effect of ubc9(93A) and hmgb3 on cell cycle and cell death. (A–E) Embryos were injected with synthetic RNAs at eight cell stage, harvested and processed at stage 33/34 (A-D), stage 35/36 (E). Injected RNAs are indicated on the left side (A–C) of each panel. Scale bar, 50 μm (A). (A–A''), (B–B'') and (C–C'') are the same section respectively. Antibodies used in immunohistochemistry are indicated above each panel (A, B, C, A', B', C'). DAPI staining (A'', B'', C''). Phospho-histone H3-positive cells (D) and apoptotic cells (E) were analyzed. Data are means ± s.e.m. (D, E). (D) $n=3$ eyes, 10 sections (lacZ), $n=3$ eyes, 10 sections (lacZ/ubc9(93A)/hmgb3) and $n=3$ eyes, 10 sections (lacZ/ubc9(93A) ($^*P=0.013$, Student's *t*-test) (E) $n=3$ eyes, 6 sections (lacZ), $n=3$ eyes, 6 sections (lacZ/ubc9(93A)/hmgb3). Asterisks indicate statistical significance determined by Student's *t*-test ($^*P<0.05$).

deficient mutant of *ubc9*, *ubc9* (*C93A*) (Nowak and Hammerschmidt, 2006). As we previously reported, upon hmgb3 overexpression, the number of embryos which exhibited enlarged eye size compared to that of *lacZ*-injected embryos modestly increased (Figs. 2A, A', E, E' and 3D) (Terada et al., 2006). While strong inhibition of ubc9 by 800 pg of *ubc9*(*93A*) injection resulted in small eyes (Supplementary Fig. S2A, B), weak inhibition of *ubc9* function by injection of a small amount of *ubc9* (*93A*) RNA (200–500 pg) did not cause a significant effect on eye development (Fig. 2B, B', F, H, H', L). Therefore, we injected 200 pg of *ubc9*(*93A*) and *hmgb3* to examine the functional interaction between ubc9(93A) and hmgb3. We observed that it was sufficient for the suppression of *hmgb3*-induced eye enlargement (Fig. 2C, C', D). More than merely suppressing eye enlargement, co-injection of *ubc9*(*93A*) and *hmgb3* caused a reduction of eye size, suggesting that hmgb3 augmented the negative effect of ubc9(93A). We then performed partial inhibition experiments of ubc9 and hmgb3 alone, or both proteins together. We previously reported that 1 pmol of *hmgb3* morpholino oligo (MO) injection results in a small eye phenotype (Terada et al., 2006). *Hmgb3* MO affects eye growth in a dose dependent manner (Supplementary Fig. S3A–C). We induced a partial inhibition of hmgb3 by injecting 0.2 pmol of *hmgb3* MO (Fig. 2G, G', J, J', K, K'). The inhibition of each protein alone did not show a significant effect (Fig. 2G, G', H, H', L), and *ubc9* (*93A*) and *control* MO did not affect eye growth (Fig. 2I, I'), however, the inhibition of both *ubc9* and *hmgb3* resulted in reduced eye size (Fig. 2J, J', L), indicating that the cooperative functioning of *ubc9* and *hmgb3* is essential for normal eye growth in *Xenopus*. This effect was rescued by the co-injection of *ubc9* (Fig. 2K, K', L). We previously demonstrated that the effect of the *hmgb3* MO was rescued by *hmgb3* RNA injection (Terada et al., 2006). These observations indicate that effects of *hmgb3* MO and *ubc9* (*93A*) were specific to each target. These results suggest that *ubc9* and *hmgb3* are functionally associated in a sumoylation activity-dependent manner to regulate eye growth.

Consensus sumoylation lysine residues are not required for functional association between ubc9 and hmgb3

We next performed *ubc9* and *hmgb3* overexpression experiments. Overexpression of both *ubc9* and *hmgb3* resulted in a high frequency of enlarged eye size (Fig. 3A–C), while overexpression of *hmgb3* or *ubc9* alone produced a weak effect on eye size (Fig. 3D, E, I). In addition, *ubc9*/*hmgb3* overexpression increased the mean eye size compared with the mean eye size of the eyes overexpressing *hmgb3* alone (Supplementary Fig. S4A). Functional cooperation between ubc9 and hmgb3 suggests that the hmgb3 protein is modified by sumoylation, leading to enhancement of progenitor proliferation. Alternatively, ubc9 may regulate eye growth by sumoylation of other target protein(s). In order to test this possibility we first examined

Fig. 5. Ubc9 and hmgb3 affect the cell cycle exit, but not cell density or cell death in the developing retina. (A–M) Embryos were injected with synthetic RNAs and harvested and processed at stage 40 (A–C, H, I, K), stage 33/34 (D), stage 32/33 (E–G), stage 41 (J, J') and stages 40/41 (L, M). Injected RNAs are indicated above (B, H, I, J), below (J', K) or on the left side (E–E'', F–F'') of each panel. Scale bar, 50 μm (A), 100 μm (E'', I). The uninjected side is indicated by "cont " (A). Nuclear density (C) and apoptotic cells (D) were analyzed. Embryos were labeled with BrdU for 1 h before harvest (E–M). (J) and (J') are the same section. Antibodies used in immunohistochemistry are indicated above each panel (E, F, E', F'). DAPI staining (A, B, E'', F''). BrdU-positive cells were analyzed (G, L, M). Arrowheads indicate BrdU-incorporating cells in the CMZ (H–J, K) and arrows indicate BrdU-incorporating cells outside the CMZ (I, J). Data are means ± s.e.m. (C, D, G, L, M). (C) $n=3$ eyes, 5 sections (cont, hmgb3/ubc9), (D) $n=3$ eyes, 8 sections (LacZ), $n=3$ eyes, 5 sections (hmgb3/ubc9), (G) $n=3$ eyes, 9 sections (lacZ), $n=3$ eyes, 9 sections (lacZ/hmgb3/ubc9), (L) $n=6$ eyes, 18 sections (lacZ), $n=4$ eyes, 12 sections (hmgb3/ubc9) ($^{**}P=0.0022$, Student's *t*-test), (M) $n=9$ eyes, 29 sections (lacZ), $n=5$ eyes, 13 sections (hmgb3/ubc9 (93A)). (N–P) Embryos were lipofected with expression construct into anterior neural region. Retinal sections were prepared at stage 41 and the numbers of EGFP-positive cells in cell clusters, which appear to be derived from a single retinal progenitor cell respectively, were counted. *EGFP*-introduced (N) and *EGFP*/*ubc9*/*hmgb3*-introduced retina (O). The average of the number of cells in each cell cluster (clone size) was calculated (EGFP: 22 retina, 478 cells; EGFP/ubc9/hmgb3: 22 retina, 499 cells) ($^*P=0.047$, Student's *t*-test) (P). Data are means ± s.e.m. re: retina ; le: lens; rpe: retinal pigment epithelium.

whether or not hmgb3 is modified by sumoylation. Hmgb3 has three lysine residues that are positioned in the consensus motif of sumoylation and one lysine residue with a high probability of sumoylation (http://www.abgent.com/doc/sumoplot; Fig. 3F). We transfected 293T cells with *ubc9*, *hmgb3* and *sumo-1* expression vectors. We did not detect significant sumoylation of hmgb3 (data not shown). We next substituted the four lysine residues of hmgb3 with arginine resides by mutagenesis to make hmgb3 (mut) (Fig. 3F). This substitution resulted in little effect on the cooperative function between ubc9 and hmgb3 for eye growth (Fig. 3C, G; Supplementary Fig. S4B). The effect of *hmgb3 (mut)* on eye enlargement was also similar to that of *hmgb3* (Fig. 3H; Supplementary Fig. S4B), suggesting

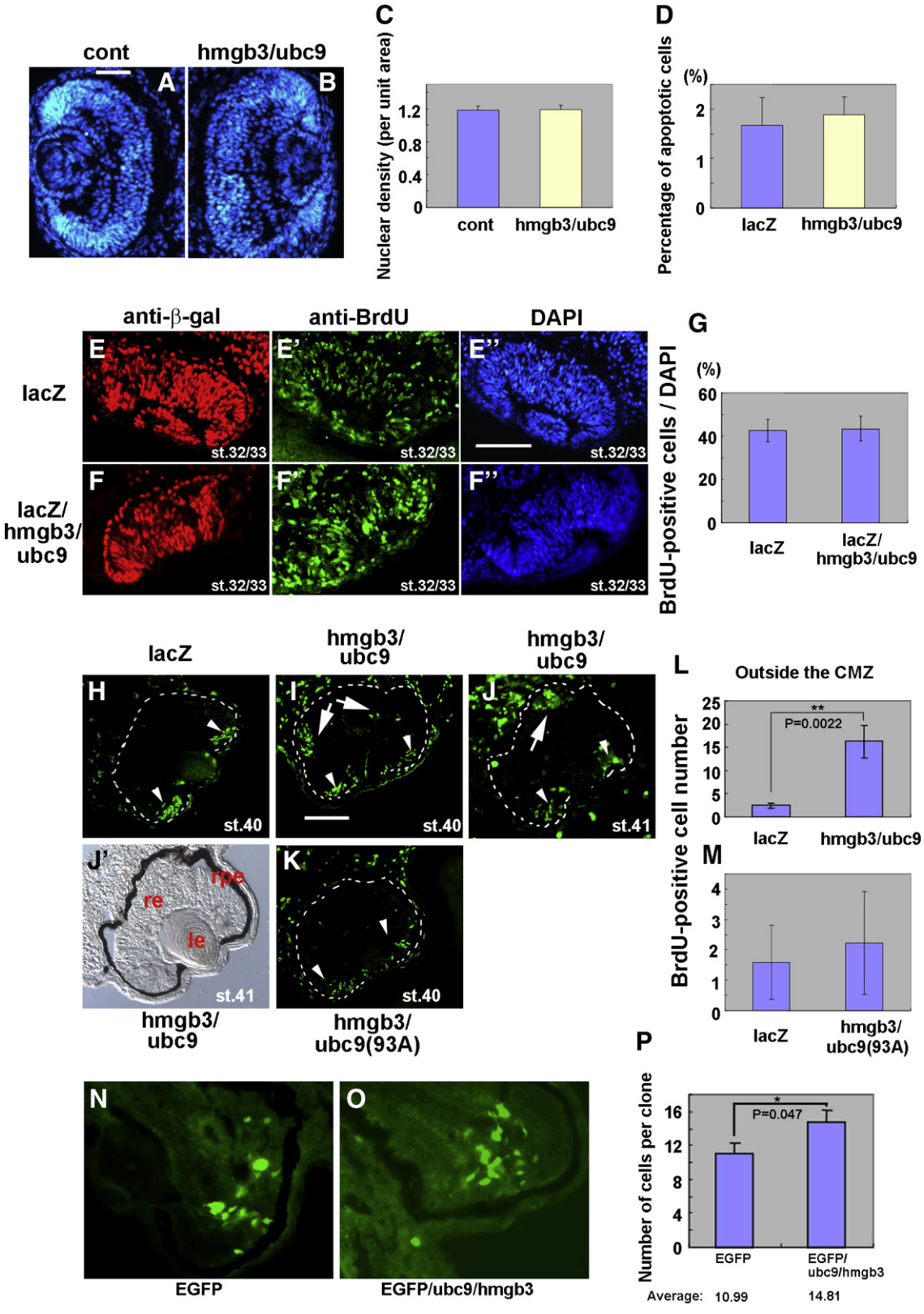

that hmgb3 is not a sumoylation target of ubc9. In order to examine if ubc9 sumoylates proteins other than hmgb3, we overexpressed ubc9, ubc9(93A), FLAG-tagged sumo-1 or HA-tagged hmgb3 in *Xenopus* embryos, followed by SDS-PAGE and Western blots. We observed an enhanced sumoylation by ubc9 overexpression (Fig. 3J). These results showed that ubc9 and hmgb3 act in an hmgb3 sumoylation-independent manner, implying that ubc9 exerts sumo-modifying actions on protein(s) other than hmgb3 to regulate eye growth.

Overexpression of ubc9 and hmgb3 suppresses cell cycle exit of retinal progenitor cells

Overexpression of both *ubc9*(*93A*) and *hmgb3* resulted in reduced eye size (Fig. 2C, C', D). We, therefore, examined whether cell cycle arrest and/or apoptosis are induced in retinal progenitors as previously reported (Nowak and Hammerschmidt, 2006). In the retina overexpressing *ubc9*(*93A*) and *hmgb3* we observed that the ratio of the number of phospho-histone H3 (pH3)-positive cells to the number of total cells in the retina increased compared to that in the *lacZ*-injected retina (Fig. 4A–B'', D), while 200 pg of *ubc9*(*93A*) alone showed little effect (Fig. 4C–C'', D), suggesting that cell cycle arrest is induced by both *ubc9*(*93A*) and *hmgb3*. We also observed an increase in the number of apoptotic cells in the retina overexpressing *ubc9*(*93A*) and *hmgb3* (Fig. 4E).

On the other hand, we observed that overexpression of *ubc9* and *hmgb3* resulted in an enlarged eye (Fig. 3A–C). The enlarged eye phenotype observed upon overexpression of both *ubc9* and *hmgb3* might be due to their effects on the formation of the eye field, cell death, cell density, and/or cell proliferation. In order to investigate this point, we examined the eye field at stage 15/16 in ubc9 & hmgb3-injected embryos, and we observed some embryos showed a subtle expansion of the eye field, while *ubc9(93A)* and *hmgb3* have little effect (*ubc9*/*hmgb3*, *rax*↑, in 5 of 14 embryos, Supplementary Fig. S5A–C). Therefore, we also examined other eye field genes, including *pax6*, *optx2* and *vsx1* (Supplementary Fig. S6). We did not observe a significant effect on those genes (Supplementary Fig. S6A–I). These observations suggest that *ubc9* and *hmgb3* overexpression does not have a significant effect on eye field formation (Supplementary Figs. S5 and S6). We then examined cell density in the retina by analyzing nuclear density, and did not observe a significant difference between injected eyes and uninjected eyes (Fig. 5A–C). We then examined cell death by TUNEL assay. We failed to observe a significant difference between the *ubc9*/*hmgb3*-overexpressed retina and the control retina (Fig. 5D). We next analyzed cell proliferation by labeling proliferating progenitor cells using BrdU. We injected *Xenopus* embryos with BrdU at stage 32/33 when almost all cells in the retina are mitotic retinal progenitors (Fig. 5E–G) (Holt et al., 1988). The ratio of the number of BrdU-positive cells to the number of total cells was not significantly different between the *ubc9*/*hmgb3*-overexpressed retina (Fig. 5F-F'', G) and the control retina (Fig. 5E–E'', G). In addition, the ratio of the number of pH3-positive cells to the number of total cells (Supplementary Fig. S9A–C) and the ratio of the number of pH3-positive cells to the number of proliferating cell nuclear antigen (PCNA)-positive cells (proliferating cells) (Supplementary Fig. S9D–H) were not significantly different between the *ubc9*/*hmgb3*-overexpressing retina and the control retina (Supplementary Fig. S9A–H). These results suggest that the cell cycle itself was not largely affected. We next labeled *Xenopus* embryos with BrdU at stage 41 when retinal development is almost completed and, therefore, proliferating progenitor/stem cells are observed only in the CMZ at this stage. We observed few proliferating cells outside the CMZ in the control retina (Fig. 5H). In contrast, we observed a significantly increased number of proliferating cells outside the CMZ in the *ubc9*/*hmgb3*-injected retina (Fig. 5I, J, J', L), suggesting that cell cycle exit of retinal progenitors is suppressed. We did not observe an increase of BrdU-positive cells in the *hmgb3*/*ubc9* (*93A*)-injected retina (Fig. 5K, M). We next examined whether *ubc9* and *hmgb3* act cell-autonomously. We lipofected *EGFP* alone or *EGFP*/*ubc9*/*hmgb3* into retinal progenitors and observed an increase in the clone size in the *EGFP*/*ubc9*/*hmgb3*-overexpressing retina compared to that observed in the *EGFP*-overexpressing retina (Fig. 5N–P), indicating that *ubc9* and *hmgb3* inhibit the cell cycle exit of retinal progenitors in a cell-autonomous manner.

We also examined the timing of when the enlarged eye phenotype manifests. We observed an enlarged eye phenotype at around stage 35/36 by visual inspection. Before stage 35/36, it is difficult to measure the eye sizes of embryos, therefore we examined the timing of the larger eye phenotype manifestation itself by whole mount *in situ* hybridization using eye marker genes, including *rax*/*Rx*, *pax6* and *six3* at earlier stages than stage 35/36. We observed that an enlargement of the eye region began after stage 28 (Supplementary Fig. S7A–O). Since it is known that retinal neurons begin to be generated after stage 26 in *Xenopus*, our observation that eye regions represented by eye marker gene expression expanded after stage 28 would be consistent with the idea that ubc9/hmgb3 affect cell cycle exit, leading to an enlarged eye phenotype.

The effect of ubc9 and hmgb3 on cell fate in the developing retina

We observed proliferating cells in the *ubc9*/*hmgb3*-overexpressing retina at stages 40/41 (Fig. 5I, J, L), and then examined whether the proliferating cells at stage 41 can differentiate into retinal neurons. We injected *Xenopus* embryos, which had been injected with *lacZ* alone or *lacZ*/*ubc9*/*hmgb3*, with BrdU at stage 41 to label proliferating cells and harvested the embryos at stage 46. We subsequently performed immunostaining of retinal sections with antibodies to BrdU and markers of retinal neurons, such as calbindin (Fig. 6A–H) or islet1 (Fig. 6I–L). We observed co-staining of BrdU and retinal markers in the *lacZ*/*ubc9*/*hmgb3*-overexpressing retina (Fig. 6A–D', K, L), but not in the *lacZ*-overexpressing retina (Fig. 6E–H, I, J), suggesting that *ubc9*/*hmgb3*-induced proliferating cells were retinal progenitor cells. We next examined whether *ubc9*/*hmgb3* affects the cell fate decision in the developing *Xenopus* retina. We did not observe a significant effect on cell fate decision by *ubc9* and *hmgb3* overexpression in the developing *Xenopus* retina (Fig. 6M, N).

Overexpression of ubc9 and hmgb3 suppresses the $p27^{Xic1}$ expression in the developing retina

Several cell cycle regulators have been reported to play significant roles in retinal development (Donovan and Dyer, 2005; Levine and Green, 2004). Among cell cycle regulators, CKI genes, including $p27^{Kip1}$, $p57^{Kip2}$, *p19*, *gadd45γ* and $p27^{Xic1}$, have been demonstrated to play significant roles in eye growth in mice and *Xenopus*. Only $p27^{Xic1}$, *p19* and *gadd45γ* genes have been identified so far in *Xenopus*. We examined the effects of ubc9 and hmgb3 on the expression of CKI genes in the retina, where the injected side was identified by EGFP fluorescence (Fig. 7A–B'). We found that while injection of *EGFP* did not affect on the expression of $p27^{Xic1}$, a CKI gene (Fig. 7C, D), $p27^{Xic1}$ expression was severely attenuated in the retina overexpressing both *ubc9* and *hmgb3* when examined by whole mount *in situ* hybridization (Fig. 7E–H) (*EGFP*, $p27^{Xic1}$↓, in 1 of 30 embryos; *EGFP*/*ubc9*/*hmgb3*, $p27^{Xic1}$↓, in 14 of 33 embryos). To confirm the attenuation of $p27^{Xic1}$ expression in the developing retina, we prepared retinal sections after whole mount *in situ* hybridization to detect $p27^{Xic1}$ expression. We observed that $p27^{Xic1}$ expression was attenuated in the developing retina overexpressing *lacZ*, *ubc9* and *hmgb3*, while not in the retina overexpressing *lacZ* alone (Fig. 7K, L). We next examined the timing of when the attenuation of $p27^{Xic1}$ expression appears upon *ubc9* and *hmgb3* overexpression. In the eye, the expression of $p27^{Xic1}$ can be detected as early as stage 26 (Ohnuma et al., 1999). Therefore, we examined the effect on $p27^{Xic1}$ at stage 25/26 and detected decreased expression of $p27^{Xic1}$ at stage 25/26 (Fig. 7M) (*EGFP*/*ubc9*/*hmgb3*, $p27^{Xic1}$↓, in 19 of 45 embryos). On the other hand, we observed that

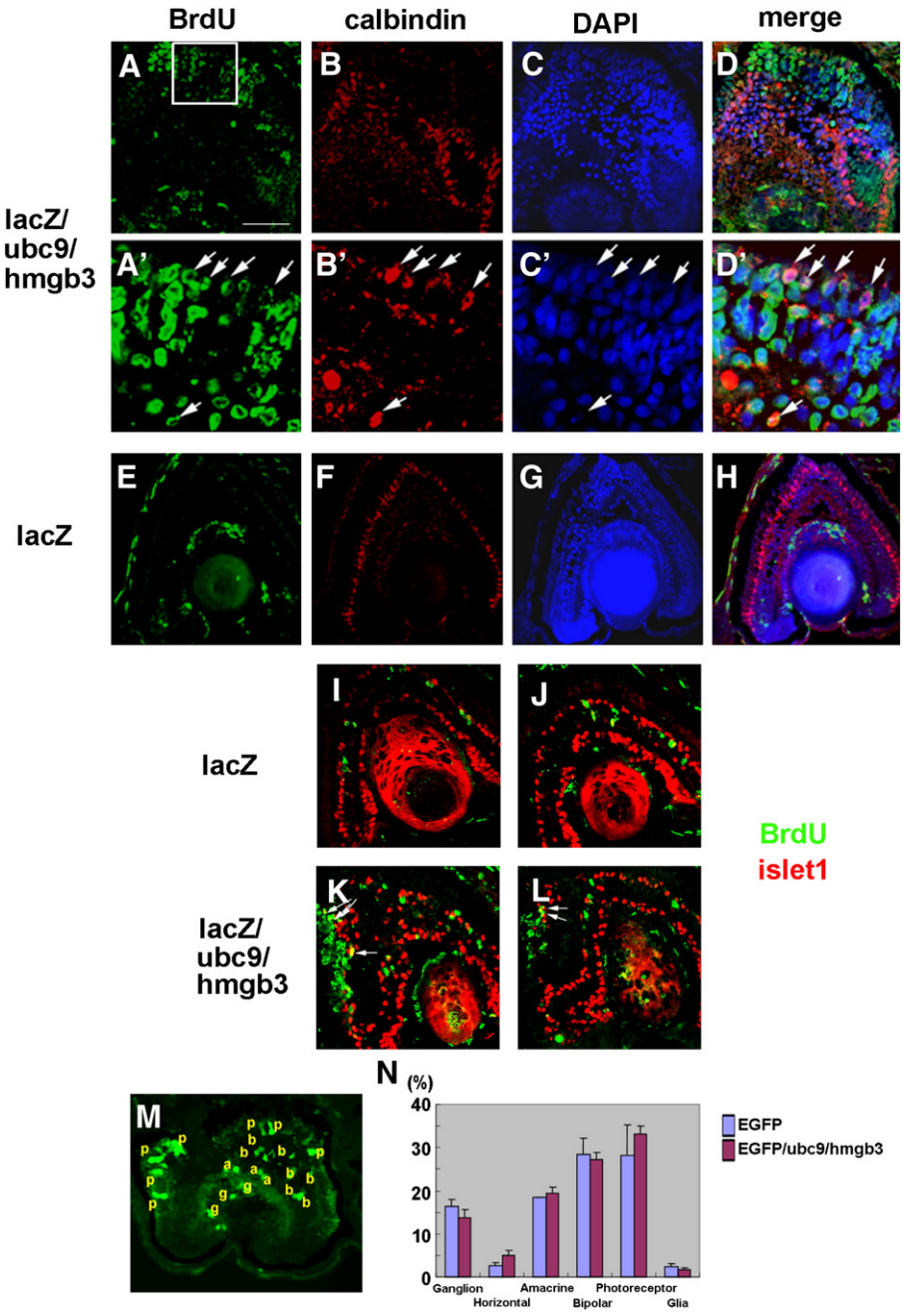

Fig. 6. The effect of ubc9 and hmgb3 on the neural potential of retinal progenitors. (A–L) Embryos were injected with *lacZ* or *lacZ*/*ubc9*/*hmgb3* RNAs at eight cell stage and then were injected with BrdU at stage 41 (A–H) or at stage 37/38 (I–L), subsequently harvested at stage 46. Antibodies used in immunohistochemistry are indicated above each panel (A, A', E), and (B, B', F). DAPI staining (C, C' G). Merge (D, D', H). Merge of BrdU signal (Green) and islet1 signal (Red) as indicated on the right of panels (I–L). Injected RNAs are indicated on the left side (A–L) of each panel. Scale bar, 100 μm (A). White arrows indicate BrdU-positive cells in (A'), calbindin-positive cells in (B'), DAPI-positive cells in (C'), and BrdU, calbindin and DAPI-positive cells in (D'), and BrdU plus islet1-positive cells in (K) and (L). (M) Retinal section (stage 41) showing EGFP-positive cells (green) lipofected with *EGFP* construct. (N) Percentage of retinal cell types observed in the retina lipofected with *EGFP* or *EGFP*/*ubc9*/*hmgb3*. $n = 591$ cells from 5 retinas for *EGFP*, $n = 638$ cells from 6 retinas for *ubc9* and *hmgb3*. Data are means ± s.e.m. p, photoreceptor cell; b, bipolar cell; g, ganglion cell; a, amacrine cell.

inhibition of both ubc9 and hmgb3 induced the precocious expression of $p27^{Xic1}$ at stage 21/22 (Fig. 7N) (*EGFP*/*ubc9(93A)*/*hmgb3*MO, $p27^{Xic1}$ ↑, in 4 of 18 embryos), although the effect from inducing $p27^{Xic1}$ expression was very small. We also examined the effect of the overexpresson of *hmgb3* alone on $p27^{Xic1}$ expression, and observed weaker effect on $p27^{Xic1}$ expression than that of *ubc9*/*hmgb3* over-expression, suggesting ubc9 can enhance the effect of hmgb3 on $p27^{Xic1}$ expression (*EGFP*/*hmgb3*, $p27^{Xic1}$↓, in 6 of 38 embryos at stage 28; *EGFP*/*ubc9*/*hmgb3*, $p27^{Xic1}$↓, in 17 of 77 embryos at stage 28). We did not observe a significant ubc9 and hmgb3 effect on the expression of cell cycle regulators including *cyclin D1*, *cyclin A2*, *cyclin B1* and *hairy2* by RT-PCR (data not shown). We also did not observe a significant difference of CKI gene *gadd45γ* expression (Fig. 7I, J, *EGFP*/*ubc9*/*hmgb3*, *gadd45γ*↓, in 1 of 20 embryos) (Decembrini et al., 2006), suggesting a selective gene regulation of CKI genes is mediated by ubc9 and hmgb3. We also examined the effect of ubc9 and hmgb3 on cell cycle inhibitor *p21* expression by quantitative-PCR using total RNAs from animal caps injected with *hmgb3* or *ubc9*/*hmgb3* (Supplementary Fig. S8). The expression of *p21* appeared to be affected by *hmgb3* or *ubc9*/*hmgb3*, although the differences of expressions of *p21* in the control were not statistically significant (Supplementary Fig. S8). These results suggest that hmgb3 and ubc9 affect *p21* expression, leading to the inhibition of

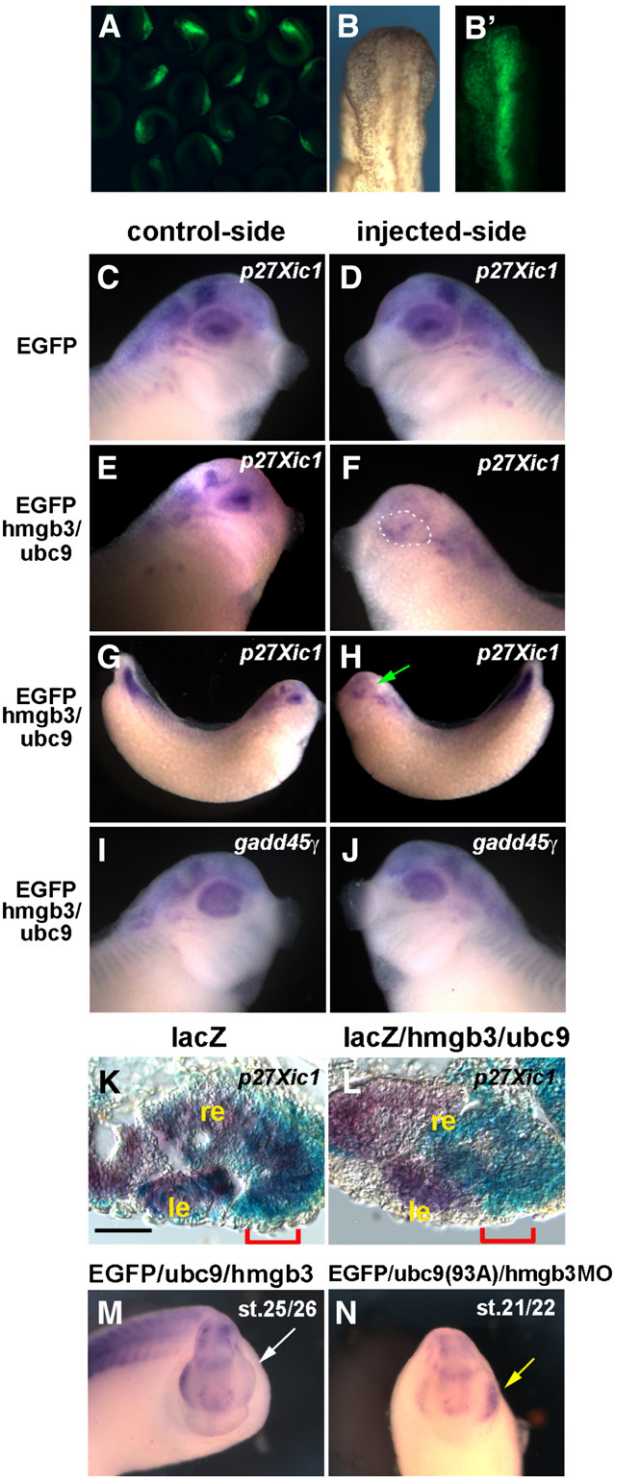

Fig. 7. *Ubc9* and *hmgb3* overexpression attenuates the expression of cell cycle inhibitor $p27^{Xic1}$. (A–B') *Xenopus* embryos injected with *EGFP* RNA. Embryos injected in the left side are collected (A). Bright field (B) and EGFP fluorescent images (B') of the same embryo injected in the left side. (C–H) *In situ* hybridization showing $p27^{Xic1}$ expression in *EGFP*- (C, D) or *EGFP*/*hmgb3*/*ubc9*- (E–H) injected embryos. Green arrow indicates the location of the eye (H). Pictures of same embryos at different magnitudes (E, G) and (F, H). (I, J) *gadd45γ* expression. Stages 32/33 (A-J). (K, L) $p27^{Xic1}$ expression in the developing retina in *Xenopus* embryos. Embryos injected with *lacZ* (K) or *lacZ*/*hmgb3*/*ubc9* (L) were harvested at stage 33/34 followed by X-gal staining. After whole mount *in situ* hybridization, cryosections were produced (K, L). Red brackets indicate regions of RNA-injection (K, L). Scale bar, 50 μm (K). Note that $p27^{Xic1}$ expression is attenuated in the RNA-injected region in (L), while not in (K). (M, N) *In situ* hybridization showing $p27^{Xic1}$ expression in *EGFP*/*ubc9*/*hmgb3*- (M) or *EGFP*/*ubc9*(*93A*)/*hmgb3MO*- (N) injected embryos. re: retina; le: lens.

the cell cycle exit of retinal progenitors. On the other hand, we failed to detect a significant signal of *p19* in the eye of *Xenopus* embryos by whole mount *in situ* hybridization (data not shown). These observations suggest that ubc9 and hmgb3 regulate cell cycle inhibitor expression.

Role of sumoylated Sp1 in retinal growth

Sumoylation of transcription factors typically induces their transcriptional repression (Gill, 2005). We examined Sp1 as a candidate target of sumoylation, since it has been reported that Sp1 has potential sites to be sumoylated and is involved in cell cycle regulation (Black et al., 2001; Spengler and Brattain, 2006; Wang et al., 2008). First, we found that *Sp1* is predominantly expressed in the developing *Xenopus* CNS, including the eye (Fig. 8A–D). Mammalian Sp1 can be sumoylated at the Lys^{16} residue (Spengler and Brattain, 2006; Wang et al., 2008), and Sp1 also has this sumoylatable Lys^{16} residue matching the sumoylation consensus residues. Therefore, we next examined whether or not *Xenopus* homolog of Sp1 can be sumoylated using 293T cells. We introduced plasmid DNAs encoding proteins of interest into 293T cells followed by SDS-PAGE and Western blot analysis (Fig. 8E, F). Sumo-modified proteins have a ~20 kDa higher molecular weight compared with unmodified proteins. We performed Western blot analysis and observed a slower migrating Sp1 (1-723) isoform, whereas we did not observe a slower migrating isoform of Sp1 (17-723) lacking the 16N-terminal amino acids containing the potential sumoylation Lys^{16} residue (Fig. 8E). These results indicate that *Xenopus* Sp1 can be sumoylated (Fig. 8F). Fusion of a sumo moiety to transcription factors mimics the effect of sumo that is covalently linked to proteins on a native lysine (Ross et al., 2002; Shalizi et al., 2006). We fused sumo-1 (1-95), which lacks the last 6 amino acids including the sumo hydrolase cleavage site, to Sp1 (17-723), creating *sumo-Sp1*. In order to investigate a functional role of *sumo-Sp1* in retinal progenitor/stem cells, we fused *sumo-Sp1* to the hormone-binding domain of glucocorticoid receptor (GRHBD), creating *sumo-Sp1-GR*, whose activity can be regulated by dexamethasone (DEX) (Fig. 8G). This system has been used to conditionally activate transcription factors during *Xenopus* embryogenesis (Suzuki and Hemmati-Brivanlou, 2000; Takebayashi-Suzuki et al., 2003). We examined the effect of *sumo-Sp1-GR* injection on eye development after stage 25-28 with DEX treatment. We observed an eye enlargement in DEX-treated embryos on the injected side (Fig. 8I, J), while not in DMSO-treated embryos (Fig. 8H, J). We next investigated the expression of $p27^{Xic1}$ in the *sumo-Sp1-GR*-injected embryos. We observed an attenuation of $p27^{Xic1}$ expression in the retina of DEX-treated embryos in the injected side (Fig. 8L, N) (*sumo-Sp1-GR*, DEX, $p27^{Xic1}$↓, in 6 of 20 embryos), while not in DMSO-treated embryos (Fig. 8K, M) (*sumo-Sp1-GR*, DMSO, $p27^{Xic1}$↓, in 0 of 12 embryos), indicating that sumo fusion of Sp1 can repress $p27^{Xic1}$ expression in the developing *Xenopus* retina. On the other hand, we observed a reduced eye phenotype in the embryos injected with un-sumoylable Sp1, Sp1(17-723)-GR, with DEX treatment, but not in those with DMSO treatment (Fig. 8O, P). We also examined the effect of *sumo-Sp1-GR* on retinal progenitor proliferation. We injected sumo-fused Sp1-overexpressing embryos with BrdU at stage 41. We observed BrdU-positive cells in the retina of DEX-treated embryos, but not in DMSO-treated embryos, outside the CMZ (Fig. 8Q–S), similar to the proliferating cells we observed in the retina of *ubc9*/*hmgb3*-injected embryos (Fig. 5I, J, L). These results suggest that sumo modification regulates the cell cycle exit of proliferating retinal progenitor cells in the developing *Xenopus*.

Roles of ubc9/hmgb3 and Sp1 in retinal growth

We performed *hmgb3* MO/*ubc9*(*93A*) or *hmgb3* MO/*ubc9*(*93A*)/*sumo-Sp1-GR* injection into embryos. We observed an almost normal eye size in embryos injected with *hmgb3* MO/*ubc9*(*93A*)/*sumo-Sp1-*

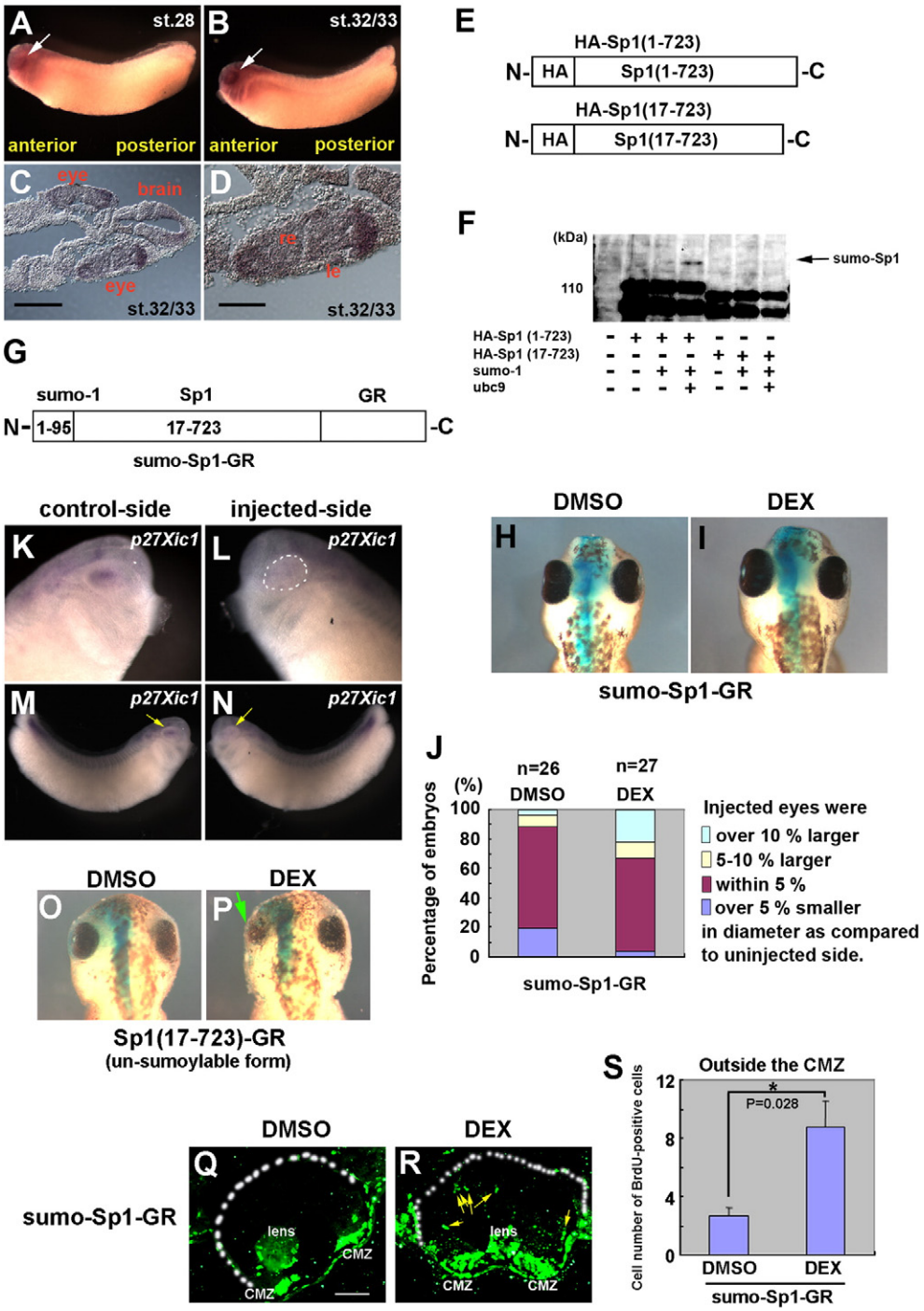

Fig. 8. *Xenopus* Sp1 is modified by sumoylation and plays a significant role in eye development. (A–D) *Sp1* expression in developing *Xenopus* at stage 28 (A) and stage 32/33 (B–D). *Sp1* expression was analyzed by whole mount *in situ* hybridization (A and B) followed by sectioning (20 μm) (C, D). *Sp1* expression is indicated by purple signal (A–D). White arrows indicate the eyes (A, B). Scale bar, 200 μm (C), 100 μm (D). (E) Structures of HA-tagged Sp1(1-723) and HA-tagged Sp1(17-723), which lacks the sumoylation target Lys (K16) residue. (F) Plasmid DNAs encoding each protein represented in (F) were introduced into 293T cells followed by SDS-PAGE and Western blot. (G) Structure of fusion protein, sumo-Sp1-GR. (H–J) *Xenopus* embryos injected with *sumo-Sp1-GR* RNA that were harvested at stage 37/38. DEX or DMSO treatment after the optic vesicle was formed (st.25-28) (H–J). Injected side is indicated by β-gal activity in blue (H, I). Differences in eye diameter between the injected side and the uninjected side were classified as indicated in the right side of (J) and the ratio of each class to the total number are indicated (J). (K–N) Embryos were injected with *sumo-Sp1-GR* RNA and harvested at stage 32/33 followed by *in situ* hybridization after collecting embryos which were injected at left side. DEX or DMSO treatment was applied after the optic vesicle was formed (st.25–28) (K–N). Same embryos are presented at different magnitudes (K, M) and (L, N). Yellow arrows indicate the location of the eyes (M, N). (O–S) Embryos were injected with synthetic RNAs, harvested and processed at stage 37/38 (O, P), stage 41 (Q–S). Injected RNAs are indicated below (O, P) or on the left side (Q, R) of each panel. DMSO or DEX treatment was applied around stage 23. DMSO-treated (O) and DEX-treated (P) embryos. Green arrow indicates reduced eye (P). Injected side is indicated by β-gal activity in blue (O, P). Embryos were labeled at stage 41 with BrdU for 1 h before harvest and subsequently immunohistochemistry was performed with anti-BrdU antibody with retinal sections (Q, R). Scale bar, 100 μm (Q). Yellow arrows indicate BrdU-incorporating cells outside the CMZ (R). Data are means ± s.e.m. (S). $n = 3$ eyes, 9 sections (DMSO), $n = 3$ eyes, 7 sections (DEX) (**$P = 0.028$, Student's *t*-test) (S).

GR (Fig. 9A), while we observed a reduced eye phenotype in embryos injected with *hmgb3MO/ubc9(93A)* (Fig. 9A). We next performed *lacZ* alone or *lacZ/ubc9/hmgb3/Sp1(17-723)-GR* injection into embryos. We observed an almost normal eye size in embryos injected with *lacZ* alone (Fig. 9B). On the other hand, we observed an enlarged eye phenotype in embryos injected with *lacZ/ubc9/hmgb3/Sp1(17-723)-*

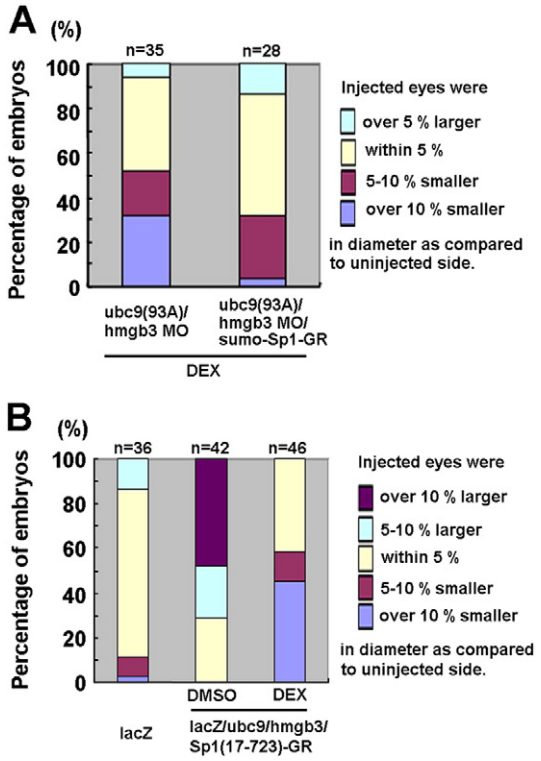

Fig. 9. The role of ubc9/hmgb3 and Sp1. (A, B) *Xenopus* embryos were injected with synthetic RNAs and/or MO as indicated below each graph (A, B), and harvested at stage 37/38 (A, B). Differences in eye diameter between the injected side and the uninjected side were classified as indicated to the right side of the graph and the ratio of each class to the total number is indicated (A, B). *Ubc9(93A)/hmgb3* MO- or *ubc9(93A)/hmgb3* MO/*sumo-Sp1-GR*-injected embryos were treated with DEX at around stage 24, and harvested at stage 37/38 (A). *lacZ/ubc9/hmgb3/Sp1(17-723)-GR*-injected embryos were divided into two groups, treated with DMSO or DEX at around stage 24, and harvested at stage 37/38 (B).

GR when the embryos were treated with DMSO (Fig. 9B). In contrast, we observed a reduced eye phenotype in embryos injected with *lacZ/ubc9/hmgb3/Sp1(17-723)-GR* when the embryos were treated with DEX (Fig. 9B). These results suggest that Sp1 acts downstream of ubc9/hmgb3 in *Xenopus* eye development.

Discussion

In this study we demonstrated that protein sumoylation activity has a significant role in the regulation of cell cycle exit in the developing *Xenopus* retina. First, *ubc9* is expressed in retinal progenitors in the developing retina and subsequently its expression is confined to the CMZ, where retinal stem cells reside. Second, co-injection of *ubc9* and *hmgb3* produced ectopic BrdU-positive dividing cells in the retina at stage 41 in a sumoylation activity-dependent manner, while BrdU-positive cells were not detected in the control retina except in the CMZ. Third, the expression of a CKI gene, $p27^{Xic1}$, was attenuated upon overexpression of *ubc9* and *hmgb3*. Fourth, we found that the *Xenopus* homolog of mammalian Sp1 can be modified by sumoylation, and sumo-fused Sp1 has a potential to negatively regulate $p27^{Xic1}$ expression.

Role of sumo modification in retinal development

Post-translational protein modifications, including phosphorylation, acetylation and ubiquitinylation have been known to act like a switch to activate or inactivate a protein or a protein complex in a cellular context-dependent manner. Recently, emerging evidence indicates that protein sumoylation modulates protein function, including the regulation of transcription factors and the subcellular localization of proteins, to control a wide variety of cellular events (Geiss-Friedlander and Melchior, 2007; Hay, 2005; Johnson, 2004). We found that *ubc9* is expressed in retinal progenitor cells. In our experiment, a prolonged expression of ubc9 and hmgb3 suppressed cell cycle exit, resulting in retinal progenitor proliferation outside the CMZ at stages 40/41 when progenitor proliferation is not normally observed. This observation suggests that protein sumoylation plays an essential role as a functional switch to control the cell cycle exit in retinal development.

The molecular events that determine the timing of "ON" and "OFF" sumo modification by affecting *ubc9* expression in the retinal progenitors have been unknown. Ubc9 expression may decrease with different speeds among progenitors. Alternatively, there may be mechanisms that allow selected cells to receive extrinsic signals, leading to the regulation of sumo modification in the cells that received the signal. However, further investigation will be required to examine these possibilities.

Role of Ubc9 in cell cycle regulation

It has been demonstrated that functions of CENP-E and TopII are controlled by sumoylation, leading to the proper regulation of chromosome segregation and subcellular localization of proteins during the G2/M phase of the cell cycle in animal cells (Dawlaty et al., 2008; Zhang et al., 2008). In zebrafish, *ubc9* is required for G2/M progression of progenitor cells in the developing retina at late developmental stages (Nowak and Hammerschmidt, 2006). However, the role of ubc9 other than cell cycle regulation of the G2/M phase has been poorly understood. It may be that cell cycle arrest at the G2/M phase in an ubc9 loss-of-function experiment makes it difficult to analyze the function of sumoylation during other phases in the cell cycle. Indeed, we also observed that *ubc9(93A)/hmgb3* overexpression appeared to confer a negative effect on eye growth.

An analysis of ubc9 functions in the cell cycle by overexpression experiments has not been reported as far as we know. We found that overexpression of *ubc9* and *hmgb3* affected BrdU uptake in retinal progenitors at stages 40/41 and also found that overexpression of *ubc9* and *hmgb3* in retinal progenitors resulted in an increase in the clone size. Considering these findings, *ubc9* may have a significant role in the control of cell cycle withdrawal in retinal progenitors.

In the hematopoietic system, hmgb3 regulates the balance between hematopoietic stem cell (HSC) self-renewal and differentiation (Nemeth et al., 2006). Hmgb3 is required for the transition of HSCs to progenitor cells, including common lymphoid progenitors and common myeloid progenitors. We observed that *hmgb3* overexpression can induce *c-myc* expression in *Xenopus* explant cultures (Terada et al., 2006). We examined whether *ubc9* can enhance *c-myc* expression induced by *hmgb3*, but we observed little effect by ubc9 on *c-myc* expression, suggesting that ubc9 regulates progenitor proliferation by a mechanism other than the regulation of *c-myc* expression (data not shown). Although we suggested that ubc9 and hmgb3 inhibit the cell cycle exit of retinal progenitor cells, it remains to be addressed whether proliferating cells at later stages (stages 40/41) overexpressing *ubc9/hmgb3* contain a population of cells possessing stem cell characteristics created by inhibiting the transition of retinal stem cells to retinal progenitors.

Role of Sp1 in retinal growth

Recently it was shown that Sp1 is sumoylated at N-terminus in mammalian cells, which negatively regulates Sp1 transcriptional activity (Spengler and Brattain, 2006). Sumoylation of Sp1 was also reported to induce translocation of Sp1 to the cytosol and to induce proteolysis of Sp1 (Wang et al., 2008). Sp1 is known to be involved in the expression of cell cycle inhibitors, including $p27^{Kip1}$ and $p21^{Cip1}$. A study using siRNA against $p27^{Kip1}$ has demonstrated that Sp1 is

required to increase the expression of $p27^{Kip1}$ through protein G kinase signaling (Cen et al., 2008). The attenuation of $p27^{Xic1}$ expression by *hmgb3* and *ubc9* overexpression in the present study may be mediated by Sp1 degradation, leading to a low level of $p27^{Xic1}$ expression, although it was not completely clear whether or not this attenuation is mediated by active repression by sumo-modified Sp1. It is known that Sp3 also recognizes the same GC-rich sequence to which Sp1 binds and that Sp3 is modified by sumoylation resulting in repression of transactivator activity (Ross et al., 2002). Our observation that the effect caused by hmgb3 and ubc9 is stronger than the effect caused by sumo fusion Sp1 mutants may suggest the existence of another target of ubc9 sumoylation in retinal development.

Interaction between hmgb3 and ubc9

Hmgb3 and *ubc9*(*93A*) overexpression caused a reduced eye phenotype, while *hmgb3* and *ubc9* overexpression resulted in an enlarged eye phenotype. In contrast, overexpression with 100 pg of *ubc9* or 200 pg of *ubc9*(*93A*) alone showed little effect on *Xenopus* eye development. Our results strongly suggest that hmgb3 augmented both the negative effect of ubc9(93A) and positive effect of ubc9 on eye growth. We also observed cell cycle arrest at the G2/M phase and apoptosis in the *ubc9*(*93A*)/*hmgb3*-overexpressing retina, but not in the retina injected with 200 pg of *ubc9*(*93A*) only. This may be due to the augmentation of ubc9(93A) function by hmgb3, as the loss-of-function of ubc9 induces cell cycle arrest and apoptosis in the developing retina (Nowak and Hammerschmidt, 2006). These results may reflect the functional interaction between hmgb3 and ubc9.

There have been studies demonstrating that a sumo E3 ligase induces cellular responses, including cell senescence, apoptosis and cell morphogenesis with ubc9 (Bischof et al., 2006; Shalizi et al., 2007). These observations raise the possibility that ubc9 may require a co-factor(s) including E3 ligase to induce these various cellular responses. Therefore, we tested the possibility that hmgb3 acts as a sumo E3 ligase. We transfected 293T cells with HA-Sp1, sumo-1, ubc9 and/or hmgb3 expression constructs. As far as we examined, we failed to obtain evidence that hmgb3 acts as a sumo E3 ligase (data not shown). Although hmgb3 does not function as an E3 ligase, we still hypothesize that hmgb3 may function as a co-factor of ubc9 to regulate retinal progenitor proliferation. In addition, our current study implies that hmgb3 and ubc9 have functional associations regulating the proliferation of progenitor/stem cells in various tissues as well. Future studies are needed for further elucidation of these hypotheses.

Acknowledgments

We thank Dr. A. Suzuki for pDH105-GRHA plasmid. We are also grateful Dr. Y. Omori for helpful discussion. We thank A. Tani, M. Kadowaki, T. Tsujii, A. Ishimaru, Y. Saioka, K. Sone, and S. Kennedy for technical assistance. This work was supported by JST. CREST, Grant-in-Aid for Scientific Research (B), Grant-in-Aid for Young Scientists (B), a Grant for Molecular Brain Science from Ministry of Education, Culture, Sports, Science and Technology, the Takeda Science Foundation, the Uehara Memorial Foundation, the Mochida Memorial Foundation, and the Naito Foundation.

Appendix A. Supplementary data

Supplementary data to this article can be found online at doi:10.1016/j.ydbio.2010.08.023.

References

al-Khodairy, F., Enoch, T., Hagan, I.M., Carr, A.M., 1995. The *Schizosaccharomyces pombe* hus5 gene encodes a ubiquitin conjugating enzyme required for normal mitosis. J. Cell Sci. 108 (Pt 2), 475–486.

Apionishev, S., Malhotra, D., Raghavachari, S., Tanda, S., Rasooly, R.S., 2001. The Drosophila UBC9 homologue lesswright mediates the disjunction of homologues in meiosis I. Genes Cells 6, 215–224.

Besson, A., Dowdy, S.F., Roberts, J.M., 2008. CDK inhibitors: cell cycle regulators and beyond. Dev. Cell 14, 159–169.

Bischof, O., Schwamborn, K., Martin, N., Werner, A., Sustmann, C., Grosschedl, R., Dejean, A., 2006. The E3 SUMO ligase PIASy is a regulator of cellular senescence and apoptosis. Mol. Cell 22, 783–794.

Black, A.R., Black, J.D., Azizkhan-Clifford, J., 2001. Sp1 and kruppel-like factor family of transcription factors in cell growth regulation and cancer. J. Cell. Physiol. 188, 143–160.

Burmeister, M., Novak, J., Liang, M.Y., Basu, S., Ploder, L., Hawes, N.L., Vidgen, D., Hoover, F., Goldman, D., Kalnins, V.I., Roderick, T.H., Taylor, B.A., Hankin, M.H., McInnes, R.R., 1996. Ocular retardation mouse caused by Chx10 homeobox null allele: impaired retinal progenitor proliferation and bipolar cell differentiation. Nat. Genet. 12, 376–384.

Casarosa, S., Amato, M.A., Andreazzoli, M., Gestri, G., Barsacchi, G., Cremisi, F., 2003. Xrx1 controls proliferation and multipotency of retinal progenitors. Mol. Cell. Neurosci. 22, 25–36.

Cayouette, M., Barres, B.A., Raff, M., 2003. Importance of intrinsic mechanisms in cell fate decisions in the developing rat retina. Neuron 40, 897–904.

Cayouette, M., Poggi, L., Harris, W.A., 2006. Lineage in the vertebrate retina. Trends Neurosci. 29, 563–570.

Cen, B., Deguchi, A., Weinstein, I.B., 2008. Activation of protein kinase G Increases the expression of p21CIP1, p27KIP1, and histidine triad protein 1 through Sp1. Cancer Res. 68, 5355–5362.

Cepko, C.L., Austin, C.P., Yang, X., Alexiades, M., Ezzeddine, D., 1996. Cell fate determination in the vertebrate retina. Proc. Natl. Acad. Sci. USA 93, 589–595.

Dawlaty, M.M., Malureanu, L., Jeganathan, K.B., Kao, E., Sustmann, C., Tahk, S., Shuai, K., Grosschedl, R., van Deursen, J.M., 2008. Resolution of sister centromeres requires RanBP2-mediated SUMOylation of topoisomerase IIalpha. Cell 133, 103–115.

Decembrini, S., Andreazzoli, M., Vignali, R., Barsacchi, G., Cremisi, F., 2006. Timing the generation of distinct retinal cells by homeobox proteins. PLoS Biol. 4, e272.

Denayer, T., Locker, M., Borday, C., Deroo, T., Janssens, S., Hecht, A., van Roy, F., Perron, M., Vleminckx, K., 2008. Canonical Wnt signaling controls proliferation of retinal stem/progenitor cells in postembryonic Xenopus eyes. Stem Cells 26, 2063–2074.

Donovan, S.L., Dyer, M.A., 2005. Regulation of proliferation during central nervous system development. Semin. Cell Dev. Biol. 16, 407–421.

Dorsky, R.I., Chang, W.S., Rapaport, D.H., Harris, W.A., 1997. Regulation of neuronal diversity in the Xenopus retina by Delta signalling. Nature 385, 67–70.

Dyer, M.A., Livesey, F.J., Cepko, C.L., Oliver, G., 2003. Prox1 function controls progenitor cell proliferation and horizontal cell genesis in the mammalian retina. Nat. Genet. 34, 53–58.

Furukawa, T., Kozak, C.A., Cepko, C.L., 1997. rax, a novel paired-type homeobox gene, shows expression in the anterior neural fold and developing retina. Proc. Natl. Acad. Sci. USA 94, 3088–3093.

Furukawa, T., Mukherjee, S., Bao, Z.Z., Morrow, E.M., Cepko, C.L., 2000. rax, Hes1, and notch1 promote the formation of Muller glia by postnatal retinal progenitor cells. Neuron 26, 383–394.

Geiss-Friedlander, R., Melchior, F., 2007. Concepts in sumoylation: a decade on. Nat. Rev. Mol. Cell. Biol. 8, 947–956.

Gill, G., 2005. Something about SUMO inhibits transcription. Curr. Opin. Genet. Dev. 15, 536–541.

Green, E.S., Stubbs, J.L., Levine, E.M., 2003. Genetic rescue of cell number in a mouse model of microphthalmia: interactions between Chx10 and G1-phase cell cycle regulators. Development 130, 539–552.

Harland, R.M., 1991. In situ hybridization: an improved whole-mount method for Xenopus embryos. Methods Cell Biol. 36, 685–695.

Harris, W.A., 2009. Retinal Development. Annu. Rev. Cell Dev. Biol.

Hay, R.T., 2005. SUMO: a history of modification. Mol. Cell 18, 1–12.

Holt, C.E., Bertsch, T.W., Ellis, H.M., Harris, W.A., 1988. Cellular determination in the Xenopus retina is independent of lineage and birth date. Neuron 1, 15–26.

Johnson, E.S., 2004. Protein modification by SUMO. Annu. Rev. Biochem. 73, 355–382.

Jones, D., Crowe, E., Stevens, T.A., Candido, E.P., 2002. Functional and phylogenetic analysis of the ubiquitylation system in *Caenorhabditis elegans*: ubiquitin-conjugating enzymes, ubiquitin-activating enzymes, and ubiquitin-like proteins. Genome Biol. 3 (RESEARCH0002).

Levine, E.M., Green, E.S., 2004. Cell-intrinsic regulators of proliferation in vertebrate retinal progenitors. Semin. Cell Dev. Biol. 15, 63–74.

Levine, E.M., Close, J., Fero, M., Ostrovsky, A., Reh, T.A., 2000. p27(Kip1) regulates cell cycle withdrawal of late multipotent progenitor cells in the mammalian retina. Dev. Biol. 219, 299–314.

Li, X., Perissi, V., Liu, F., Rose, D.W., Rosenfeld, M.G., 2002. Tissue-specific regulation of retinal and pituitary precursor cell proliferation. Science 297, 1180–1183.

Marquardt, T., Ashery-Padan, R., Andrejewski, N., Scardigli, R., Guillemot, F., Gruss, P., 2001. Pax6 is required for the multipotent state of retinal progenitor cells. Cell 105, 43–55.

Mathers, P.H., Grinberg, A., Mahon, K.A., Jamrich, M., 1997. The Rx homeobox gene is essential for vertebrate eye development. Nature 387, 603–607.

Nacerddine, K., Lehembre, F., Bhaumik, M., Artus, J., Cohen-Tannoudji, M., Babinet, C., Pandolfi, P.P., Dejean, A., 2005. The SUMO pathway is essential for nuclear integrity and chromosome segregation in mice. Dev. Cell 9, 769–779.

Nemeth, M.J., Kirby, M.R., Bodine, D.M., 2006. Hmgb3 regulates the balance between hematopoietic stem cell self-renewal and differentiation. Proc. Natl. Acad. Sci. USA 103, 13783–13788.

Nieuwkoop, P.D., Faber, J., 1994. Normal table of *Xenopus laevis* (Daudin). Garland, New York.
Nowak, M., Hammerschmidt, M., 2006. Ubc9 regulates mitosis and cell survival during zebrafish development. Mol. Biol. Cell 17, 5324–5336.
Ohnuma, S., Philpott, A., Wang, K., Holt, C.E., Harris, W.A., 1999. p27Xic1, a Cdk inhibitor, promotes the determination of glial cells in Xenopus retina. Cell 99, 499–510.
Onishi, A., Peng, G.H., Hsu, C., Alexis, U., Chen, S., Blackshaw, S., 2009. Pias3-dependent SUMOylation directs rod photoreceptor development. Neuron 61, 234–246.
Ross, S., Best, J.L., Zon, L.I., Gill, G., 2002. SUMO-1 modification represses Sp3 transcriptional activation and modulates its subnuclear localization. Mol. Cell 10, 831–842.
Seufert, W., Futcher, B., Jentsch, S., 1995. Role of a ubiquitin-conjugating enzyme in degradation of S- and M-phase cyclins. Nature 373, 78–81.
Shalizi, A., Gaudilliere, B., Yuan, Z., Stegmuller, J., Shirogane, T., Ge, Q., Tan, Y., Schulman, B., Harper, J.W., Bonni, A., 2006. A calcium-regulated MEF2 sumoylation switch controls postsynaptic differentiation. Science 311, 1012–1017.
Shalizi, A., Bilimoria, P.M., Stegmuller, J., Gaudilliere, B., Yang, Y., Shuai, K., Bonni, A., 2007. PIASx is a MEF2 SUMO E3 ligase that promotes postsynaptic dendritic morphogenesis. J. Neurosci. 27, 10037–10046.
Sherr, C.J., Roberts, J.M., 1999. CDK inhibitors: positive and negative regulators of G1-phase progression. Genes Dev. 13, 1501–1512.
Spengler, M.L., Brattain, M.G., 2006. Sumoylation inhibits cleavage of Sp1 N-terminal negative regulatory domain and inhibits Sp1-dependent transcription. J. Biol. Chem. 281, 5567–5574.
Suzuki, A., Hemmati-Brivanlou, A., 2000. Xenopus embryonic E2F is required for the formation of ventral and posterior cell fates during early embryogenesis. Mol. Cell 5, 217–229.
Takebayashi-Suzuki, K., Funami, J., Tokumori, D., Saito, A., Watabe, T., Miyazono, K., Kanda, A., Suzuki, A., 2003. Interplay between the tumor suppressor p53 and TGF beta signaling shapes embryonic body axes in Xenopus. Development 130, 3929–3939.
Taylor, K.M., Labonne, C., 2005. SoxE factors function equivalently during neural crest and inner ear development and their activity is regulated by SUMOylation. Dev. Cell 9, 593–603.
Terada, K., Kitayama, A., Kanamoto, T., Ueno, N., Furukawa, T., 2006. Nucleosome regulator Xhmgb3 is required for cell proliferation of the eye and brain as a downstream target of Xenopus rax/Rx1. Dev. Biol. 291, 398–412.
Van Raay, T.J., Moore, K.B., Iordanova, I., Steele, M., Jamrich, M., Harris, W.A., Vetter, M.L., 2005. Frizzled 5 signaling governs the neural potential of progenitors in the developing Xenopus retina. Neuron 46, 23–36.
Wallace, V.A., 2008. Proliferative and cell fate effects of Hedgehog signaling in the vertebrate retina. Brain Res. 1192, 61–75.
Wang, Y.T., Chuang, J.Y., Shen, M.R., Yang, W.B., Chang, W.C., Hung, J.J., 2008. Sumoylation of specificity protein 1 augments its degradation by changing the localization and increasing the specificity protein 1 proteolytic process. J. Mol. Biol. 380, 869–885.
Watanabe, M., Takahashi, K., Tomizawa, K., Mizusawa, H., Takahashi, H., 2008. Developmental regulation of Ubc9 in the rat nervous system. Acta Biochim. Pol. 55, 681–686.
Young, R.W., 1985. Cell differentiation in the retina of the mouse. Anat. Rec. 212, 199–205.
Zhang, X.D., Goeres, J., Zhang, H., Yen, T.J., Porter, A.C., Matunis, M.J., 2008. SUMO-2/3 modification and binding regulate the association of CENP-E with kinetochores and progression through mitosis. Mol. Cell 29, 729–741.
Zuber, M.E., Perron, M., Philpott, A., Bang, A., Harris, W.A., 1999. Giant eyes in *Xenopus laevis* by overexpression of XOptx2. Cell 98, 341–352.